Is It Possible to Characterize the Geometry of a Real Porous Medium by a Direct Measurement on a Finite Section? 1: The Phase-Retrieval Problem[1]

Yannick Anguy,[2] Robert Ehrlich,[3] and Cédric Mercet[2]

Macroscopic transport properties of natural porous media, such as the permeability tensor $\underset{\approx}{K}$, are the sum of uncountable microscopic events. Understanding how these microscopic events come together to yield a descriptive *property, such as $\underset{\approx}{K}$, is facilitated if a set of porous descriptors $P_{i=1,N}^i$ can be measured that synthesize all the critical microscopic properties of a real porous medium and that can be related to the computed $\underset{\approx}{K}$. The main difficulty lies in choosing the correct $P_{i=1,N}^i$. A description of the microgeometry of a porous medium by a set of $P_{i=1,N}^i$ will be declared adequate if synthetic numerical porous media generated from the $P_{i=1,N}^i$ possess the same $\underset{\approx}{K}$ as the real medium. This paper is another step for creating such synthetic porous media. The candidate geometrical descriptor P^1 considered herein is the autocorrelation function (ACF) measured directly on a sample of finite size v included in a porous medium of size V; $V \gg v$. Capitalizing on the phase retrieval problem (retrieving an object from knowledge of its Fourier modulus) encountered in general imaging, it is shown that there exists a one-to-one relation between a digital thin section and its ACF. This is demonstrated using an iterative procedure, the* Error Reduction/Hybrid Input Output *algorithm, that allows one to recover uniquely, to within a pixel, a finite image from its ACF. A theoretical implication of this is that a direct measurement on a finite image cannot characterize the geometry of a porous medium. Yet, in stochastic modeling, quasi-infinite numerical porous media are commonly generated from acquired ACF. Such quasi-infinite stochastic porous media must include a structural noise as a practical consequence of the unicity of the relation between an image and its ACF. To correctly interpret the relation between $\underset{\approx}{K}$ and the microgeometry, it becomes necessary to verify that this nonimposed structural noise does not control the output $\underset{\approx}{K}$ of the numerical simulations.*

---

[2]Laboratoire Energétique et Phénomènes de Transfert, UMR CNRS No. 8508, Esplanade des Arts et Métiers, 33405 Talence cedex, France; e-mail: yannick@lept-ensam.u-bordeaux.fr
[3]Residuum Energy, 1048 S. Oak Hills Way, Salt Lake City, Utah 84108.

NOMENCLATURE

Roman Letters

$A_{\beta\sigma}$ — Interfacial area of the β-σ interface associated with the closure problem (Eq. (4)), e.g., contained within the REV, m^2

$A_{\beta\sigma}$ — Interfacial area of the β-σ interface contained within the macroscopic system, m^2

$A_{\beta e}$ — Area of entrances and exits for the β-phase contained within the macroscopic system, m^2

$\underset{\sim}{d}$ — Vector field, m. The closure variable $\underset{\sim}{d}$ is related in the β-phase to the microscopic spatial deviation pressure $\dot{p}_\beta$ according to $\dot{p}_\beta = \underset{\sim}{d} \cdot (\nabla <p_\beta>^\beta - \rho_\beta \underset{\sim}{g})$ (Quintard and Whitaker, 1994c). The spatial deviation pressure $\dot{p}_\beta$ is defined according to Gray's decomposition of length scales: $p_\beta = <p_\beta>^\beta + \dot{p}_\beta$ (Gray, 1975).

$\underset{\approx}{D}$ — Second-order tensor field, m^2. The closure variable $\underset{\approx}{D}$ is related to the microscopic velocity $\underset{\sim}{v}_\beta$ according to $\underset{\sim}{v}_\beta = 1/\mu_\beta \underset{\approx}{D} \cdot (\nabla P <p_\beta>^\beta - \rho_\beta \underset{\sim}{g})$ (Barrère, Gipouloux, and Whitaker, 1992; Quintard and Whitaker, 1994c)

$\underset{\sim}{g}$ — Gravity vector, $m \cdot s^{-2}$

$\underset{\approx}{I}$ — Unit tensor

$\underset{\approx}{K}$ — Traditional DARCY's law permeability tensor, m^2

1_i — Lattice vector for a unit cell, m

l_β — Characteristic length-scale for the β-phase at the microscopic scale, m

l_σ — Characteristic length-scale for the σ-phase at the microscopic scale, m

L_p — Characteristic length-scale for the volume averaged pressure gradient $\nabla <p_\beta>^\beta$, m (Quintard and Whitaker, 1994b)

L_v — Characteristic length-scale for the volume averaged velocity $<\underset{\sim}{v}_\beta>^\beta$, m (Quintard and Whitaker, 1994b)

L_ε — Characteristic length-scale for the porosity, m (Quintard, and Whitaker, 1994b)

p_β — Pressure in the β-phase, $N \cdot m^{-2}$

$\dot{p}_\beta$ — $p_\beta - <p_\beta>^\beta$: Spatial deviation pressure in the β-phase (Gray, 1975; Quintard and Whitaker, 1994b), $N \cdot m^{-2}$

$<p_\beta>^\beta$ — Intrinsic volume averaged pressure, $N \cdot m^{-2}$ (Quintard and Whitaker, 1994a)

r_m	Characteristic length of the averaging volume (REV), m
$\underset{\sim\beta}{r}$	Position vector locating points in the β-phase, m
$\underset{\sim\beta}{v}$	Velocity vector in the β-phase, m·s^{-1}
$<\underset{\sim\beta}{v}>$	Superficial volume averaged velocity, m·s^{-1} (Quintard and Whitaker, 1994a)
V	Volume of the averaging volume, m^3
V_β	Volume of the β-phase contained in the averaging volume, m^3

Greek Letters

μ_β	Viscosity of the β-phase, N·s·m^{-2}
ρ_β	Mass density of the β-phase, kg·m^{-3}
$\zeta(\underset{\sim\beta}{r}, t)$	Arbitrary vector used as a reminder of what one does not know, m·s^{-1}. In general the boundary condition at $A_{\beta e}$ is known only in terms of averages (Prat, 1990)

Subscripts
β Fluid phase
σ Solid phase

Mathematical Operators/Symbols

$<>$ Superficial volume average operator: $<\psi_\beta>|_{\underset{\sim}{x}} = \frac{1}{V}\int_{V_\beta(\underset{\sim}{x})} \psi_\beta(\underset{\sim}{x} + \underset{\sim}{y})\, dV_y$

$<>^\beta$ Intrinsic volume average operator: $<\psi_\beta>^\beta|_{\underset{\sim}{x}} = \frac{1}{V_\beta}\int_{V_\beta(\underset{\sim}{x})} \psi_\beta(\underset{\sim}{x} + \underset{\sim}{y})\, dV_y$

$\otimes$ Convolution product

GENERAL CONTEXT

Porous rocks such as sandstones and carbonates consist of a solid matrix riddled with voids, the porosity. The porosity consists of pores connected by pore throats as well as such stress-related features as fractures and microfractures. This paper is one in a series that describes our attempts to fundamentally understand flow behavior in unfractured porous sandstones with both a single fluid and mutually immiscible fluid phases. The problem must be attacked from a modeling point of view based on strong empirical evidence. The properties of fluids (e.g., viscosity, density, electrical conductivity, etc.) are well known. Until recently this was not the case with respect to the porous medium. It has been accepted as a truism that in sandstones the porosity consists of small bodies (pores) connected by pore throats (Bakke and Oren, 1997; Kwiecien, Macdonald, and Dullien, 1990; Thovert, Sallés, and Adler, 1992). The porous microstructure consists of a three-dimensional array of pores of various sizes and shapes connected by pore throats with a variety of sizes. The rules that control the degree of order of this array and the rules that

control the assignment of throat sizes to adjacent pores (the porous microstructure) are the controlling parameters of the porosity with respect to flow (Berg, 1975; Graton and Fraser 1935; Prince, Ehrlich, and Anguy, 1995). Over the past decade it has been shown that the porosity exposed on a two-dimensional slice through a sandstone carries sufficient information to predict permeability and other properties with high precision both statistically and in terms of packing theory (Ehrlich and others, 1991a,b; McCreesh, Ehrlich, and Crabtree, 1991). Thus the conventional petrographic thin section contains critical structural information concerning the three-dimensional microstructure; or such three-dimensional physical properties could not be determined (Ehrlich and others, 1991b). The aforementioned studies have shown the utility of using Fourier transforms of the binary (pores = 1, matrix = 0) thin section images to obtain structural parameters (Anguy and others, 1994; Prince, Ehrlich, and Anguy, 1995). This then leads to an approach for creating a synthetic model medium that has all of the critical properties of a real, observed, porous medium (Anguy, Bernard, and Ehrlich, 1996). This paper represents another step in that effort.

The need for such a model lies in our grand objective of understanding the fundamentals of flow through a porous medium. A property such as permeability is a *descriptive* property (a *volume average*) with no physical explanation. It is the sum of an uncountable microscopic events that are described in the STOKES' equations. One of our major objectives is to understand how such microscopic events come together to yield the macroscopic permeability.

Our approach to this goal is the change of scale technique which relies on direct numerical simulation on the pore scale. The change of scale technique may be expressed in a number of ways: the homogeneization theory (Bensoussan, Lions, and Papanicolaou, 1978; Sanchez-Palencia, 1980), the stochastic approach (Dagan, 1979, 1990; Gelhar, 1984; Matheron, 1965), the Brownian approach (Brenner, 1980), the variational procedure (Rubinstein, and Torquato, 1989), and the volume-averaging technique (Anderson and Jackson, 1967; Marle, 1967; Quintard and Whitaker, 1993, 1994a–e; Slattery, 1967; Whitaker, 1967). We concentrate on the volume-averaging technique illustrated herein for the process of single-phase flow of an isovolume fluid through a rigid medium. The change of scale approach relies on the existence of a natural scale, r_m, the Representative Elementary Volume scale (REV), below which the microscopic point equations and boundary conditions apply and above which the geometry of the solid matrix and the void space can be averaged and replaced by a fictitious continuum at the macroscopic scale (Bachmat and Bear, 1986; Weathcraft, Sharp, and Tyler, 1990). Averaging the microscopic point balance equations over an REV yields from first principles the macroscopic equations governing the phenomena at the continuum scale. Volume averaging the STOKES' equations (1) governing the process of single phase flow through a porous medium on the microscopic scale yields the macroscopic DARCY's law, Equation (2), governing the process at the continuum scale.

$$-\nabla p_\beta + \mu_\beta \nabla^2 \underset{\sim}{v}_\beta = \underset{\sim}{0}$$

$$\nabla \cdot \underset{\sim}{v}_\beta = 0$$

$$\text{B.C.1: } \underset{\sim}{v}_\beta = \underset{\sim}{0} \quad \text{on} \quad A_{\beta\sigma} \tag{1}$$

$$\text{B.C.2: } \underset{\sim}{v}_\beta = \zeta(\underset{\sim}{r}_\beta, t) \quad \text{on} \quad A_{\beta e}$$

$$<\underset{\sim}{v}_\beta> = -\frac{1}{\mu_\beta} \underset{\approx}{K} \cdot \left(\underset{\sim}{\nabla} <p_\beta>^\beta - \rho_\beta \underset{\sim}{g} \right) \tag{2}$$

where p_β and $\underset{\sim}{v}_\beta$ are the point pressure and velocity vector fields in the fluid phase (the state variables on the microscopic scale); $<\underset{\sim}{v}_\beta>$ and $<p_\beta>^\beta$ are the superficial volume averaged velocity and intrinsic volume averaged pressure (the state variables on the macroscopic scale).

The natural scale r_m required for the theoretical derivation of DARCY's law is associated with the length-scale constraints expressed by Equations (3a) and (b) (Dagan, 1979; Tartar, 1980; Whitaker, 1969, 1986):

$$l_\beta, l_\sigma \ll r_m \tag{3a}$$

$$r_m^2 \ll L_\varepsilon L_p \tag{3b}$$

$$r_m^2 \ll L_\varepsilon L_v$$

where l_β, l_σ are characteristic lengths for the fluid phase (β) and solid phase (σ) on the microscopic scale. Equation (3a) refers to the requirement that a geometrical REV exists, and it expresses that the size of the averaging volume must be large with respect to the length scales representative of the pore-scale to smooth the effects of the microscopic heterogeneities (Bear, 1972; Marle, 1967; Pilotti, 1998). L_ε, L_p and L_v are characteristics length-scales for the porosity ε_β, the volume averaged pressure gradient $\underset{\sim}{\nabla} <p_\beta>^\beta$, and the volume averaged velocity $<\underset{\sim}{v}_\beta>^\beta$, respectively. Equation (3b) expresses that significant variations in averaged quantities (ε_β, $<\underset{\sim}{v}_\beta>^\beta$ and $\underset{\sim}{\nabla} <p_\beta>^\beta$) occur over distances ($L_\varepsilon$, L_v, and L_p, respectively) that are large compared to the size r_m of the averaging volume (Carbonell, and Whitaker, 1984; Nozad, Carbonell, and Whitaker, 1985). When Equations (3a) and (b) are valid, the different scales (the pore-scale and the continuum scale) may be decoupled with each scale having its specific state variables; the state variables at the continuum level consisting of filters of the state variables on the pore level, Equations (1–2), (Cushman, 1990). In DARCY's law, Equation (2), the constitutive variable $\underset{\approx}{K}$ (permeability tensor) appearing at the continuum scale is interpreted as a *place holder* replacing the loss of information about the details of the microgeometry when moving from a pore-scale description to a continuum

description (Cushman, 1990). Thus, information propagation over scales can be studied.

Furthermore, when Equations (3a) and (b) are valid, the REV can be treated as a unit cell in a spatially periodic porous medium and a *closure problem* can be developed, Equation (4), at the microscopic scale, over the unit cell, whose solution yields the permeability tensor $\underset{\approx}{K}$ Equation (5), appearing in DARCY's law (Barrère, Gipouloux, and Whitaker, 1992).

$$-\underset{\sim}{\nabla}\underset{\sim}{d} + \nabla^2\underset{\approx}{D} = \underset{\approx}{I}$$

$$\underset{\sim}{\nabla} \cdot \underset{\approx}{D} = \underset{\sim}{0}$$

$$\underset{\approx}{D} = \underset{\sim}{0} \quad \text{at} \quad A_{\beta\sigma} \tag{4}$$

$$\text{Periodicity: } \underset{\approx}{D}(\underset{\sim}{r} + l_i) = \underset{\approx}{D}(\underset{\sim}{r}); \quad \underset{\sim}{d}(\underset{\sim}{r} + l_i) = \underset{\sim}{d}(\underset{\sim}{r})$$

$$\text{Average: } <\underset{\sim}{d}>^\beta = \underset{\sim}{0}$$

$$-\frac{\varepsilon_\beta}{V_\beta} \int_{V_\beta} \underset{\approx}{D} \, dV = -\varepsilon_\beta <\underset{\approx}{D}>^\beta = \underset{\approx}{K} \tag{5}$$

The form of the closure problem demonstrates theoretically that $\underset{\approx}{K}$ is an implicit function $\underset{\approx}{f}$ of the microgeometry Equation (6). So that knowledge of the microgeometry allows to calculate rigorously $\underset{\approx}{K}$ by direct simulation on the microscopic level. Equations (1–5) provide the most general physical/mathematical model for evaluating a flow property at the REV-scale as an implicit function of microscopic properties.

$$\underset{\approx}{K} = \underset{\approx}{f} \text{ (microgeometry)} \tag{6}$$

In this context, availability of realistic input geometries is a prerequisite. Detailed input geometries may be directly obtained from modem techniques such as combined X-ray tomography and high-intensity synchrotron X-ray sources (Ferreol, and Rothman, 1995) or serial sectioning (Kwiecien, Macdonald, and Dullien, 1990). Yet, the *filtered* output $\underset{\approx}{K}$ of the simulation Equation (5), is very difficult to relate directly to the input geometry in the form of a 3D discrete image consisting of about 10^9 solid or fluid *voxels* (volume elements). Such a way of computing transport properties lacks predictive power (Garboczi, 1990). To improve our understanding of the relation between microscopic properties and macroscopic flow properties ($\underset{\approx}{K}$), it remains to express Equation (6) as a predictive and ultimately analytical model. As outlined by Equations (7–9), this demands the identification

of a minimal set of porous descriptors $P_{i=1,N}^i$ synthesizing the characteristics of the geometry and that can be related to the output $\underset{\approx}{K}$ (Garboczi, 1990).

$$\text{microgeometry} = g\left(P_{i=1,N}^i\right) \tag{7}$$

$$\underset{\approx}{K} = \underset{\approx}{h}\left(P_{i=1,N}^i\right); \qquad \left(P_{i=1,N}^i\right) \subseteq \left(P_{i=1,N}^i\right) \tag{8}$$

$$d\underset{\approx}{K} = \sum_{i=1}^{N} \frac{\partial \underset{\approx}{h}}{\partial p^i} \, dp^i \tag{9}$$

Relation (7) expresses that the geometry is completely characterized through an implicit function g by a set of parameters $P_{i=1,N}^i$. $\underset{\approx}{K}$ is then characterized through an implicit function $\underset{\approx}{h}$ by a subset of parameters $P_{i=1,N}^i$ included in the set $P_{i=1,N}^i$ and describing the part of the geometry relevant to $\underset{\approx}{K}$ [Eqs. (8-9)]. In Equation (9), $\Sigma_{i=1}^N \partial \underset{\approx}{h}/\partial p^i$ is an intrinsic function of the model used to predict $\underset{\approx}{K}$ (Anguy, Bernard, and Ehrlich, 1996).

In this framework, the main difficulty lies in choosing the appropriate $P_{i=1,N}^i$. See van Brakel (1975), Dullien (1979), Quiblier (1984), and Renard and de Marsily (1997) for partial bibliographies of the topic. As expressed by the intuitive constraint (3a), the averaging volume theory requires the existence of a geometrical REV, i.e., a sample of minimal size encompassing all the geometrical characteristics in a homogeneous porous medium. If the input geometry does not include a geometrical R.E.V., $\underset{\approx}{K}$ is shown to include microscopic fluctuations not represented by DARCY's law and a nonlocal theory must be developed (Quintard, and Whitaker, 1990). The determination of the geometrical REV should rely on the properties of a set of acquired porous descriptors $P_{i=1,N}^i$. The description of a porous medium by the set of $P_{i=1,N}^i$ will be declared appropriate if synthetic numerical porous media possessing similar transport properties ($\underset{\approx}{K}$) than the real medium can be generated from $P_{i=1,N}^i$.

In a number of applications, it is necessary to simulate the physical behavior of the medium on a scale larger than the scale attached to the geometrical characterization. To comply with this requirement, synthetic porous media should be formed by the *replication* of a large number of geometrical REVs. Synthetic media showing this property are temed *quasi-infinite* porous media. Herein, *quasi-infinite* synthetic porous media are needed because, in the change of scale, the concept of REV implies that the macroscopic medium is periodic, Equation (4). Natural media are not strictly periodic. Previous analyses of sandstones using Fourier transforms showed that this class of porous medium is *quasiperiodic* (Prince, and Ehrlich, 1990; Prince, Ehrlich, and Anguy, 1995). In this, one periodicity assumption implicit in the change of scale method can be met. *Quasiperiodicity* in this sense implies the existence of a degree of randomness at scales greater than

the geometrical REV. Yet, the region required for solution must contain enough geometrical REVs to faithfully express the random component of natural media (Anguy, Bernard, and Ehrlich, 1994).

This paper focuses on whether or not a set of $P_{i=1,N}^i$ measured directly on a sample of finite size can characterize the geometry of a porous medium. Such $P_{i=1,N}^i$ as a *measure* of a geometrical REV, should permit one to formulate and solve practical problems related to the estimation of the geometry in unsampled areas of the porous medium: $P_{i=1,N}^i$ are meant to be fitted in a process yielding *quasi-infinite* numerical porous media. This issue will be covered in forthcoming contributions.

INTRODUCTION

A porous medium may be viewed as the consequence of a general process varying in time and space. In the case of geological media (rocks), such process may include depositional processes (hydrodynamics, bioturbation), early postdepositional processes and postlithification processes (pressure solution, tectonic deformation). A porous medium exists in a well-defined region of space, denoted by $V(x, y, z)$, whose boundaries ∂V depend upon the length scale and time scale of the aforementioned causal processes. In practice, porous media are studied only over a finite portion $v(x, y, z)$ of $V(x, y, z)$ whose boundaries ∂v, size v ($v \ll V$), and position depend often, if not always, upon practical, logistic, or economic considerations (Bryant, King, and Mellor, 1993). As far as we are concerned, the sampling window $v(x, y, z)$ may be either a polished section of a few cm^2 imaged by a Scanning Electron Microscope (SEM) (Fig. 1 for example) or a 3D sample of a few mm^3 imaged by combined X-ray tomography and high-intensity synchrotron X-ray sources.

The objective of the paper is to answer the general question: is it possible to characterize the geometry of a real porous medium of geometrical support $V(x, y, z)$ by a set of parameters $P_{i=1,N}^i$ measured directly on a binarized digital image of finite size v? Our objective is worth stating precisely: one does not address a stereological ambiguity of type it is possible to characterize the microgeometry of a 3D porous medium by 2D parameters? and the question to be answered can be expressed as: is it possible to characterize the geometry of an nD porous medium by a set of nD descriptors $P_{i=1,N}^i$ measured directly on an nD digital sample of finite size? The argumentation developed hereafter is 2D but remains valid whatever the dimension of the porous object is, to the extent that the dimension of the object is ≥ 2 (Sault, 1984). A set of $P_{i=1,N}^i$ allowing to answer by the affirmative should meet the following requirements:

1) all the information about geometrical features, as they are expressed in the finite image $v(x, y)$ should be carried by the porous descriptors, $P_{i=1,N}^i$,

2) the $P_{i=1,N}^i$ as a *measure* of a geometrical REV should not depend upon position (Quintard, and Whitaker, 1987).
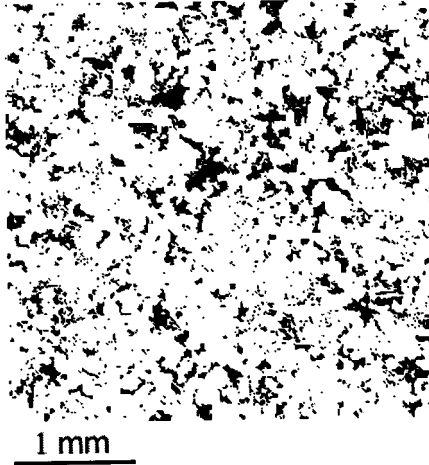
Figure 1. 256 × 256 binary (0–1) digital image from a sandstone sample portraying pixels of one class (in our case porosity) by one single intensity (1) expressed by black and the remainder (rock matrix) by another intensity (0).

The parameter, P^1, considered in this work is the 2D autocorrelation function (ACF) measured on a binarized image of finite support v (x, y) (Fig. 2). Verifying that no geometrical information is omitted when using the ACF as porous descriptor necessitates that the nature and the quantity of information carried by the ACF be controlled. A general solution may consist in identifying the geometrical features of a finite image (Fig. 1) that can be recovered from its ACF (Fig. 2). An analogy is first drawn between the latter solution and the *phase retrieval problem* (retrieving an object from knowledge of its Fourier modulus) encountered in a number of seemingly disparate areas (crystallography, optics, wave front sensing, or astronomy). Capitalizing on work in the aforementioned areas, a practical solution to recovering geometrical features of an image of finite size v is then proposed in the form of a numerical iterative procedure referred to as the *Error Reduction/Hybrid Input Output* algorithm. The iterative procedure is outlined and illustrated by a computer experiment which allows one to recover, to within a pixel, uniquely and systematically the image in Figure 1 from its ACF (Fig. 2). In a last part, the consequences of this fundamental result are discussed along two lines:

- the theoretical side: is it possible to characterize the geometry of a homogeneous porous medium of size V by a direct measurement on an image of finite size v; v ≪ V?
- the practical side: is it appropriate to use a measured ACF for generating the *quasi infinite* porous media required by the general framework outlined by Equations (6–9)?
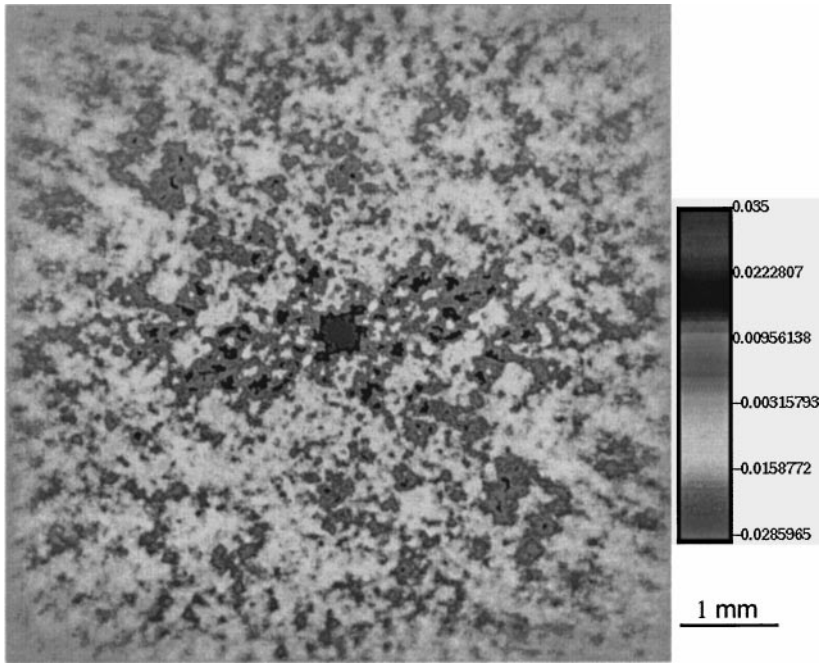
Figure 2. Two-dimensional ACF measured on Figure 1. In this display, the ACF is *centered* and normalized by the variance $\sum_{i=0}^{N-1} \sum_{j=0}^{N-1} (h(iT, iT) - \varepsilon_\beta)^2$ ε^β: porosity). The normalized ACF is commonly interpreted as characterizing the dependence of a point $(iT + r_x, jT + r_y)$ upon a point (iT, jT) (Ventzel, 1973) (see graylevel map legend). Lag $r_x = 0, r_y = 0$, is located at the center of the display. Horizontal lags r_x (resp. vertical lags r_y) range from left to right (respectively bottom to top) from $-N \times T$ to $+N - 1 \times T$, e.g., -3474 to $+3460$ μm ($N = 256$ and $T = 13.57$ μm). So as to see the small peaks of the normalized ACF, all values $\geq 3.5 \cdot 10^2$ and ≤ 1 are represented in the same gray level (see graylevel map legend). Figure 2 highlights a universal characteristic of nomalized ACF functions: a big peak at small lags, of maximum value equal to 1 at lag (0, 0), which decreases rapidly towards 0. By means of the discrete correlation theorem, the ACF is calculated in the Fourier domain (Eqs. (12–15)) capitalizing on False Fourier Transform algorithms.

MATHEMATICAL BACKGROUND

A binary image of type Figure 1 may be described by the discrete phase function $h(x, y)$ expressed by Equation (10):

$$h(x, y) = \sum_{k=0}^{N-1} \sum_{i=0}^{N-1} h(kT, lT) \, \delta(x - kT, y - lT) \tag{10}$$

where T is the sampling interval in each local Cartesian direction ($T = 13.57$ μm in Figure 1) and δ is the Dirac distribution (Roddier, 1985). The discrete phase

function $h(x, y)$ comprises $N \times N$ samples portraying pixels of one class (in our case porosity) by one single intensity (1) and the remainder (rock matrix) by another intensity (0) ($N = 256$ in Fig. 1). $h(x, y)$ is identically null out of a finite support of size $NT \times NT$.

The discrete ACF $\sigma(r_x, r_y)$ may be calculated in the object domain as

$$\sigma(r_x, r_y) = \sum_{i=0}^{N-1} \sum_{j=0}^{N-1} h(iT, jT)h(iT + r_x, jT + r_y);$$

$$r_x, r_y = 0, \pm T, \pm 2T, \ldots, \pm(N-1)T. \tag{11}$$

By means of the discrete correlation theorem, the ACF may be equally calculated in the Fourier domain, Equations (12–15). The discrete Fourier transform implying periodicity in both object- and Fourier-domain, the digital image (Fig. 1) is represented by a periodic infinite wave-form, $h_{pi}(x, y)$, Equation (12), whose unit cell $h_e(x, y)$ is obtained by appending zeros to the original $N \times N$ image. The size $T_e \times T_e$ of the period, equal to $N_e T \times N_e T$, is justified a little further on.

$$h_{pi}(x, y) = h_e(x, y) \otimes \left(T_e^2 \sum_{r=\infty}^{+\infty} \sum_{s=\infty}^{+\infty} \delta(x - rT_e, y - sT_e) \right) \tag{12}$$

The periodic infinite discrete density Fourier power spectrum $|H_{pi}(\nu_x, \nu_y)|^2$ of Equation. (12) is:

$$|H_{pi}(\nu_x, \nu_y)|^2 = |H(\nu_x, \nu_y)|^2 \times \left(\sum_{m=-\infty}^{+\infty} \sum_{n=-\infty}^{+\infty} \delta\left(\nu_x - \frac{m}{T_e}, \nu_y - \frac{n}{T_e}\right) \right) \tag{13}$$

where ν_x, ν_y are horizontal and vertical wave-numbers and where the individual period $|H(\nu_x, \nu_y)|^2$ is calculated as

$$|H(\nu_x, \nu_y)|^2 = \left| \sum_{k=0}^{N_e-1} \sum_{l=0}^{N_e-1} h_e(kT, lT) \, e^{-2\pi j(\nu_x kT + \nu_y lT)} \right|^2 \tag{14}$$

By means of the discrete correlation theorem, the inverse Fourier transform of $|H_{pi}(\nu_x, \nu_y)|^2$ (Eq. (13)) yields the discrete periodic ACF $\sigma_{pi}(r_x, r_y)$, Equation (15):

$$\sigma_{pi}(r_x, r_y) = \sigma(r_x, r_y) \otimes \left(T_e^2 \sum_{m=-\infty}^{+\infty} \sum_{n=-\infty}^{+\infty} \delta(x - mT_e, y - nT_e) \right) \qquad (15)$$

The sampling theorem states that unless the period $T_e = N_e T$ of the *zero-extended* sequence $h_e(x, y)$ is chosen such that $N_e \geq 2N - 1$, when we make the inverse Fourier transform of the two members of Equation (13), we find that the ACF $\sigma_{pi}(r_x, r_y)$ of the periodic infinite image is an *aliazed* ACF corresponding to the $2N - 1 \times 2N - 1$ ACF of the unit cell $\sigma(r_x, r_y)$ convolved by an array of δ whose spacing is T_e in each direction (Brigham, 1974; Pérez-Ilzarbe, 1992). Here N_e is chosen equal to $2 \times N$ as illustrated in Figure 1 by the dotted square representing the boundaries of the *zero-appended* unit cell $h_e(x, y)$.

THE PHASE RETRIEVAL PROBLEM

As mentioned above, appropriateness for a measured ACF to characterize the geometry of a porous medium depends partly on the requirement that no information should be lost about geometrical features, as they are expressed in the image. A general approach to quantifying the information carried by the ACF may consist of identifying the geometrical features of the image that can be recovered from the ACF. To do so, one may capitalize on the *phase retrieval problem* which appeared in the context of general imaging where it is often convenient to measure the Fourier transform of an object rather than the object itself and where it often happens that it is impossible to measure the phase $\varphi(\nu_x, \nu_y)$ of the Fourier transform accurately (Millane, 1990). A finite image being uniquely defined by the inverse Fourier transform (FT[1]) of its Fourier transform $H(\nu_x, \nu_y)$, Equation (16), the phase $|\varphi(\nu_x, \nu_y)|$ must be known if one is to reconstruct the image. Thus recovering an image from its measured Fourier modulus $|H(\nu_x, \nu_y)|$ is a *phase problem* (Millane, 1990).

$$h_e(x, y) = FT^{-1}(H(\nu_x, \nu_y)); \quad H(\nu_x, \nu_y) = |H(\nu_x, \nu_y)|e^{j\varphi(\nu_x,\nu_y)} \qquad (16)$$

On the basis of the discrete correlation theorem (Eqs. (12–15)), the ACF of a finite image can be derived straightforwardly from the Fourier amplitude $|H(\nu_x, \nu_y)|$, using only mathematical operators. In this case, $|H(\nu_x, \nu_y)|$ and $\sigma(r_x, r_y)$ contain the same information. Then, recovering a finite image from its ACF $\sigma(r_x, r_y)$ is frequently referred to as the *phase retrieval problem* since it is equivalent to determining the phase of an image when given only its Fourier

modulus $|H(\nu_x, \nu_y)|$ (Sault, 1984; Schultz, and Snyder, 1992; Nieto-Vesperinas, 1993).

There are essentially three issues concerned with the reconstruction of an object from its ACF (Kim, and Hayes, 1990):

    i) the uniqueness of the solution; the *ambiguity* (existence of multiple solutions) of the *phase retrieval problem* from a theoretical point of view,

    ii) the development of algorithms for recovering an object from the ACF, the numerical side, and

    iii) the sensitivity of the reconstructions to noise or measurement errors.

Here, one addresses the numerical side. The iterative algorithm used hereafter borrows from the Gerchberg–Saxton algorithm (Gerchberg and Saxton, 1972; Saxton, 1978) and is due to Fienup (1982). This algorithm, referred to as the *Error Reduction/Hybrid Input Output algorithm*, has been already covered (Fienup, 1982; Fienup, and Wackerman, 1986) but is summarized below for completeness.

A NUMERICAL SOLUTION TO THE PROBLEM OF RECOVERING A FINITE IMAGE FROM ITS ACF

A kth iteration of the Error Reduction algorithm consists of the four simple steps represented in Figure 3.

    1) Fourier transform a current estimate $g_k(x, y)$ of the image to be recovered.

    2) Make the minimum changes in the computed Fourier transform $G_k(\nu_x, \nu_y)$ which allow it to satisfy the Fourier constraints, e.g., replace the Fourier modulus of the computed $G_k(\nu_x, \nu_y)$ by the measured Fourier modulus $|H(\nu_x, \nu_y)|$ to form $G'_k(\nu_x, \nu_y)$, an estimate of the Fourier transform of the object $H(\nu_x, \nu_y)$. The Fourier constraint $|H(\nu_x, \nu_y)|$ is calculated from the measured ACF (Eqs. (12–15)).

    3) Invert Fourier transform $G'_k(\nu_x, \nu_y)$ to form $g'_k(x, y)$.

    4) Make the minimum changes in $g'_k(x, y)$ which allow it to satisfy weak object-domain constraints to form a new estimate $g_{k+1}(x, y)$ of the object. In Fienup (1982) iterative Error Reduction algorithm, the fourth step is performed as expressed in Figure 3, where γ is the set of points at which $g'_k(x, y)$ violates the object-domain constraints, i.e., wherever $g'_k(x, y)$ exceeds the known *diameter* of the object computed as half the *diameter* of the ACF. γ is the set of points that fall out a square mask of size $NT \times NT$ representing an upper bound of the true support of the object (Fig. 1) (Pérez-Ilzarbe, Nieto-Vesperinas, and Navarro, 1990).

The iterations continue until the computed Fourier transform $G_k(\nu_x, \nu_y)$ satisfy the Fourier domain constraints and/or the computed image $g'_k(x, y)$ satisfy
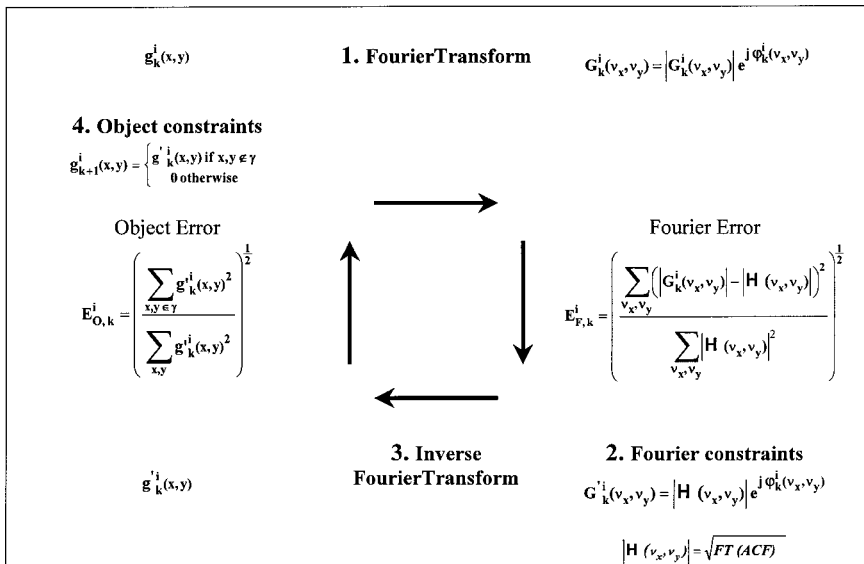
$g_k^i(x,y)$ **1. FourierTransform** $G_k^i(v_x,v_y) = \left| G_k^i(v_x,v_y) \right| e^{j\varphi_k^i(v_x,v_y)}$

4. Object constraints

$g_{k+1}^i(x,y) = \begin{cases} g_k'^i(x,y) \text{ if } x,y \in \gamma \\ 0 \text{ otherwise} \end{cases}$

Object Error

$$E_{O,k}^i = \left(\frac{\sum_{x,y \in \gamma} g_k'^i(x,y)^2}{\sum_{x,y} g_k^i(x,y)^2} \right)^{\frac{1}{2}}$$

Fourier Error

$$E_{F,k}^i = \left(\frac{\sum_{v_x,v_y} \left(\left| G_k^i(v_x,v_y) \right| - \left| H(v_x,v_y) \right| \right)^2}{\sum_{v_x,v_y} \left| H(v_x,v_y) \right|^2} \right)^{\frac{1}{2}}$$

$g_k'^i(x,y)$

**3. Inverse
FourierTransform**

2. Fourier constraints

$G_k'^i(v_x,v_y) = \left| H(v_x,v_y) \right| e^{j\varphi_k^i(v_x,v_y)}$

$\left| H(v_x,v_y) \right| = \sqrt{FT(ACF)}$

Figure 3. Fienup's iterative processing loop for recovering an image from its measured ACF and an estimate of the image support. In 2D and 3D, the exact support of the object is not known and so the *diameter* constraints is not applied tightly (Fienup, 1982).

the object-domain constraints (Fienup, 1982). The convergence of the algorithm is monitored by calculating a Fourier domain error $E_{F,k}$ and/or an object-domain error $E_{O,k}$ explicited in Figure 3. In practice, the Error Reduction algorithm converges slowly (Gerchberg, and Saxton, 1972; Saxton, 1978). A solution to the slow convergence of the Error Reduction algorithm is the Hybrid Input–Output algorithm which differs with the Error Reduction algorithm only with respect to the fourth step in Figure 3 performed as expressed by Equation (17) (Fienup, 1982):

$$g_{k+1}(x, y) = \begin{cases} g_k'(x, y) & \text{if} \quad (x, y) \notin \gamma \\ g_k(x, y) - \beta g_k'(x, y) & \text{if} \quad (x, y) \in \gamma \end{cases} \tag{17}$$

In an iteration of type Hybrid Input-Output, the input function $g_k(x, y)$ is no longer an estimate of the object and can be thought as the driving function for the next output $g_k'(x, y)$ (Fienup, 1982). In Equation (17), β is a constant feedback parameter ranging typically between 0.1 and 1 (Lane, 1987; Sault, 1984).
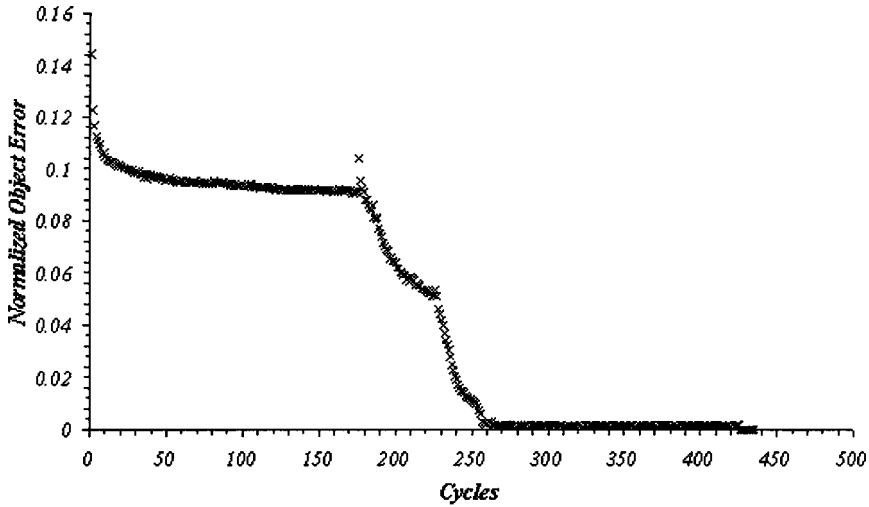
Figure 4. Normalized object error $E'_{O,k}$ vs. the number of cycles i for the problem of phase retrieval using the ER/HIO algorithm of Fienup (1982). The starting point for the algorithm is a realization of a normally distributed random field with zero mean and unit variance. β(Eq. (17)) is kept constant equal to 0.7 all along the experiment.

A COMPUTER SIMULATION EXAMPLE

In this section, we show a computer experiment using the iterative *Error Reduction (ER)/Hybrid Input Output (HIO) algorithm* for recovering the 256 × 256 image in Figure 1 from its ACF (Fig. 2). The initial guess for the image is an any 256 × 256 realization of a normally distributed random field. Figure 4 shows a plot of the normalized object error $E^i_{O,k}$ [Eq. (18)] vs. the number of cycles i.

$$E^i_{O,k} = \left(\frac{\sum\limits_{x,y \in \gamma} \left(g''^i_k(x, y)\right)^2}{\sum\limits_{x,y} \left(g''^i_k(x, y)\right)^2} \right)^{1/2} \tag{18}$$

where subscript k represents the last iteration in each cycle.

The *Error Reduction/Hybrid Input Output algorithm* is first used with a maximum number of 175 cycles with each cycle comprising nine HIO iterations followed by three ER iterations ($k = 12$ in Eq. (18)). In the first six iterations of cycle one, the correct 256 × 256 square mask defining the object-domain

constraints is replaced with a reduced-area triangular mask. Indeed, a real image $h(x, y)$ and its mirror $h(-x, -y)$ have the same ACF, so that features of both images may be reconstructed simultaneously resulting, sometimes, in a stable condition of *stagnation* for the algorithm. The reduced support favors some of the features of either $h(x, y)$ or $h(-x, -y)$ over the other, allowing the algorithm to converge towards that image after reinstating the correct support constraint (Fienup, and Wackerman, 1986). Figures 5–7 display the estimates g_{12}^1, g_{12}^{25}, and g_{12}^{175} of the image after cycles 1, 25, and 175, respectively. At cycle 175 the current reconstruction g_{12}^{175} (Fig. 7) is not the searched image so that g_{12}^{175} is used as initial guess for a series of 50 more cycles (176–225), each comprising 25 HIO iterations followed by seven ER iterations. The first 10 iterations in the series of cycles involve a reduced support yielding the increase of the error $E_{O,32}^{176}$ (Fig. 4). Figure 8 shows the current reconstruction g_{32}^{185} at cycle 185. In Figure 8, geometrical features of the searched image become distinguishable. The object error $E_{O,32}^{225}$, being not zero after these additional cycles, g_{32}^{225} is used as starting point for a series of 200 more cycles (cycles 226–425) comprising 50 HIO iterations and 10 ER iterations. The error $E_{O,60}^i$ decreases rapidly towards an asymptotic value of about 15×10^{-4} (Fig. 4) suggesting that we are faced with a stagnation problem on an image close to the true object but with differences. These differences are illustrated in Figure 9, where the current estimate g_{60}^{325} is shown to include a pattern of stripes of low contrast superimposed upon
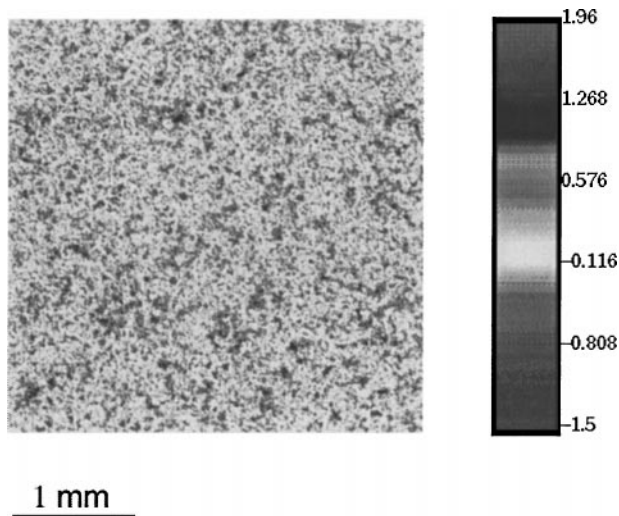

Figure 5. Estimate g_{12}^1 of the image to be recovered (Fig. 1) after cycle one. The object error, $E_{O,12}^1$ is equal to 0.144. See graylevel map for the values of the pixels comprising the estimate.
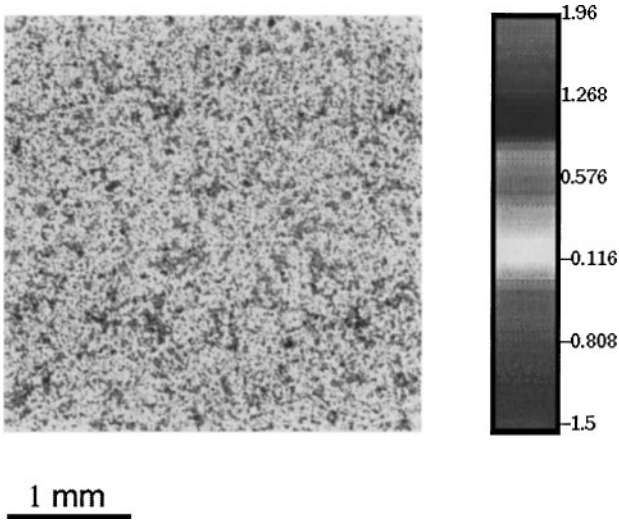
1 mm

Figure 6. Estimate g_{12}^{25} obtained at cycle 25 ($E_{O,12}^{25} = 0.100$).

the image; stripes extend outside the 256×256 support of the object, so that the error metric cannot be zero implying that a striped image is not a solution and do not represent a uniqueness problem (Fienup, and Wackerman, 1986). Successful methods for overcoming stagnation associated with stripes are covered in
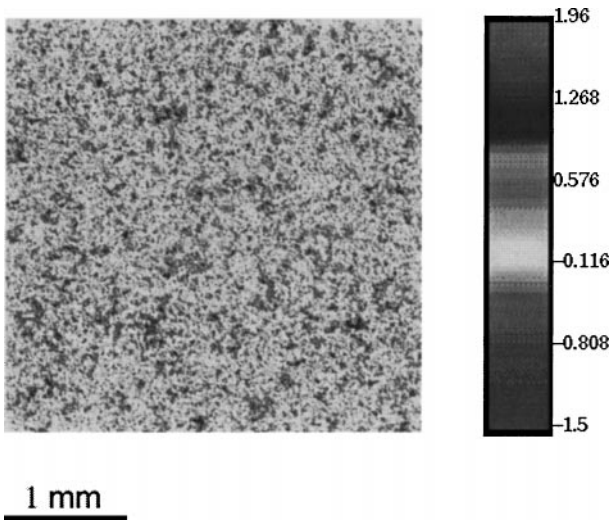

1 mm

Figure 7. Estimate g_{12}^{175} after cycle 175 ($E_{O,12}^{175} = 0.092$).
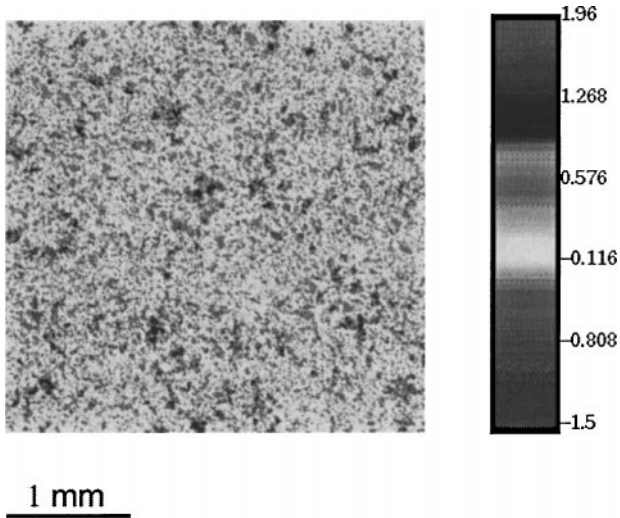
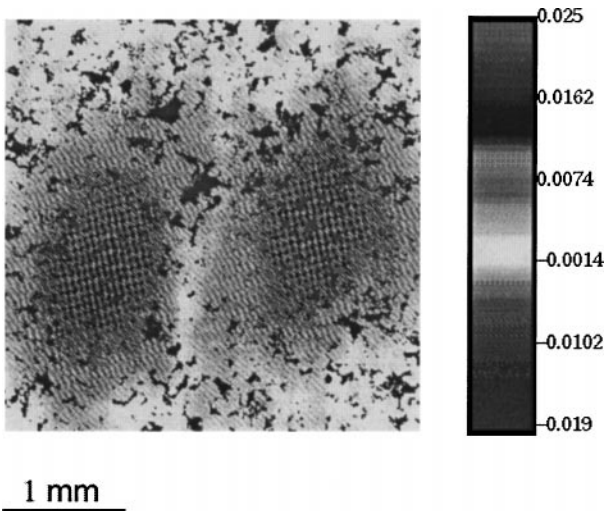**Figure 8.** Estimate g_{32}^{185} after cycle 185 ($E_{O,32}^{185} = 0.086$).

Figure 9. Estimate g_{60}^{325} after cycle 325 ($E_{O,60}^{325} = 0.0015$). All pixel values ≥ 0.025 and ≤ 1.02266 and all pixel values ≥ -0.025 and ≤ -0.019 are represented with constant gray level (see graylevel map legend), highlighting a pattern of stripes of low contrast.
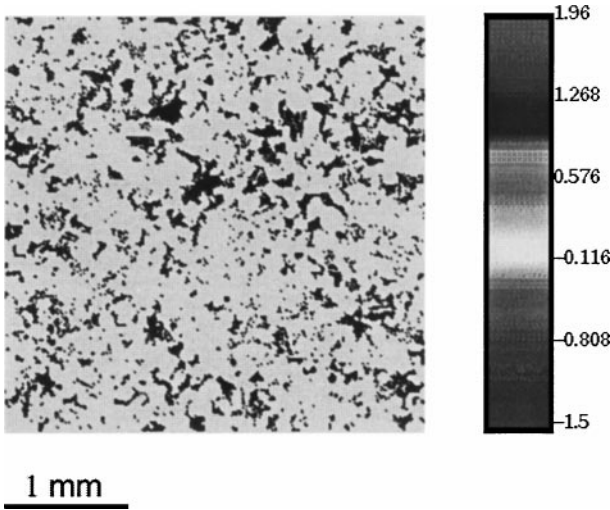
Figure 10. Estimate g_{275}^{435} after cycle 435 ($E_{0,275}^{435} = 2.10^{-7}$).

Fienup and Wackerman (1986). Here, 10 last more cycles (each 200 HIO iterations followed by 75 ER iterations) are sufficient to escape the local minimum associated with stripes. Figure 10 represents the image g_{275}^{435} at cycle 435 with an associated error metric of $2.\,10^{-7}$. The reconstructed image is exactly the image in Figure 1.

   Starting from different initial inputs, we reconstructed systematically, to within a pixel, the image in Figure 1 (and all the images we tried). Figure 11 shows a convergence curve obtained using as the starting point another normally distributed random sequence. The same binary image being reconstructed each time, one can have confidence that there are no multiple solutions to recovering an object from its ACF. Of course *trivial ambiguities* may be solutions such as $h(-x, -y)$, $h(x - x_1, y - y_1)$ as all these functions possess the same ACF (Lane, 1987; Millane, 1990; Sault, 1984). Such *trivial ambiguities* are not considered as multiple solutions.

   In this work only 2D binary images were considered. Extension to 3D is straightforward. However, the 1D case is very different and contains inherent multiple solutions (Sault, 1984). Mention also that, almost often, an additional nonnegative constraint in the object domain is imposed on $g_k'(x, y)$ to make $g_{k+1}(x, y)$ (Fienup, 1982; Pérez-Ilzarbe, Nieto-Vesperinas, and Navarro, 1990; Sasaki, and Yamagami, 1987; Sault, 1984; Schultz, and Snyder, 1992). Such constraint of positivity was not taken into account in this work.
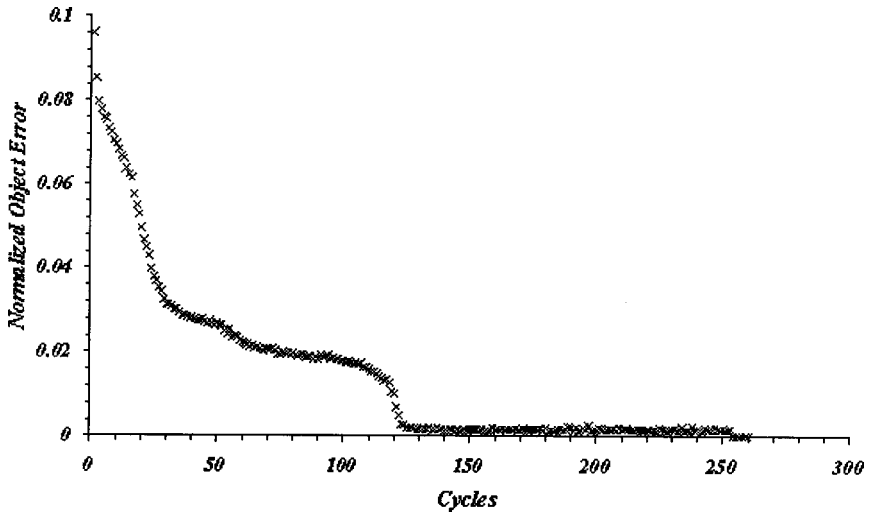
Figure 11. Normalized object error $E'_{O,k}$ vs. the number of cycles i for the problem of phase retrieval using as starting point another normally distributed random realization.

DISCUSSION AND CONCLUSIONS

Theoretical Consequences

Using the iterative *Error Reduction/Hybrid Input Output algorithm*, we reconstructed, to within a pixel, uniquely and systematically a binary image from the only knowledge of its ACF. In this respect, we showed that there exits a *one-to-one* (bijective) relation between a binary image of finite size v and its ACF $\sigma(r_x, r_y)$. This demonstrates numerically the necessary condition C.1 for answering by the affirmative to the question raised in the title.

C.1. The ACF carries all the information about the geometrical features comprised in the finite support v (x, y)

A sufficient condition may then be expressed as C.2:

C.2.

    i) C. 1, and

    ii) the ACF measured on a set of M finite supports v $(x_j, y_j)_{j=1,M}$ included in V is a geometrical invariant, i.e., the ACF does not depend upon position.

Obviously, C. 2 cannot be verified. Indeed, consider a series of M sampling windows v $(x_j, y_j)_{j=1,M}$ in a porous medium. Such a series may represent a set of thin sections. Denoting by $\sigma^j(r_x, r_y)$ the ACF measured on the jth support v (x_j, y_j)

we have, as a consequence of the unicity of the pair "binary image/ACF"

$$\sigma^1(r_x, r_y) \neq \sigma^2(r_x, r_y) \neq \cdots \neq \sigma^j(r_x, r_y) \cdots \neq \sigma^M(r_x, r_y) \qquad (19)$$

otherwise the M finite sections would be exactly the same, to within a pixel. Inability for the ACF to characterize the geometry of M sections means inability to characterize the geometry of the porous medium. This is sufficient to answer by the negative to the question raised in the title: a direct measurement on a digital image of finite size cannot be used as a *measure* of a geometrical REV.

A geometrically homogeneous porous medium may be defined in the manner of Quintard and Whitaker (1987):

D.1. A porous medium of size V is homogeneous with respect to a window of size v (v ≪ V) if all its geometrical measurements do not depend upon position.

In accordance with the existence of homogeneous porous media and the unicity of the pair "binary image/ACF," the following model is proposed for the measured ACF:

$$\sigma^1(r_x, r_y) = \sigma^{\text{intrinsic}}(r_x, r_y) + \delta\sigma^1(r_x, r_y)$$

$$\cdots$$

$$\sigma^j(r_x, r_y) = \sigma^{\text{intrinsic}}(r_x, r_y) + \delta\sigma^j(r_x, r_y) \qquad (20)$$

$$\cdots$$

$$\sigma^M(r_x, r_y) = \sigma^{\text{intrinsic}}(r_x, r_y) + \delta\sigma^M(r_x, r_y)$$

where $\sigma^{\text{intrinsic}}(r_x, r_y)$ is a *measure* of a geometrical REV in a homogeneous porous medium. $\sigma^{\text{intrinsic}}(r_x, r_y)$ may be interpreted as a probabilistic descriptor of the structure of the natural process at the origin of the rock. $\delta\sigma^j(r_x, r_y)$ is a deterministic quantity expressing the influence of the finiteness of the boundaries $\partial v(x_j, y_j)$ of the sampled window v (x_j, y_j). $\delta\sigma^j(r_x, r_y)$ expresses "that the finite image v (x_j, y_j) is isolated in a unique manner *in an infinite field of zeros*" (Matheron, 1965, 1970). The finite boundaries $\partial v(x_j, y_j)$ are not *impassable*: the calculation of $\sigma^j(r_x, r_y)$ passes through the finite boundaries $\partial v(x_j, y_j)$ (Eq. (11) or (15)). In this respect, $\delta\sigma^j(r_x, r_y)$ expresses deterministic *edge effects* and is related only to the finite image v (x_j, y_j). Through $\delta\sigma^j(r_x, r_y)$, $\sigma^j(r_x, r_y)$ contains too much information and cannot be considered as independent of the finite field it is measured on. To that extent, $\sigma^j(r_x, r_y)$ cannot be used to solve problems related to the prediction of the geometry. The unknown $\sigma^{\text{intrinsic}}(r_x, r_y)$ is the relevant parameter. Yet, the passage from $\sigma^j(r_x, r_y)$ to the simpler $\sigma^{\text{intrinsic}}(r_x, r_y)$ remains an unsolved problem (Matheron, 1965, 1970).

Practical Consequences

We examined if $\sigma(r_x, r_y)$, measured directly on a finite support $v(x, y)$, can represent a *measure* of a geometrical REV in a homogeneous medium of size $V \gg v$. In searching for such a *measure* of the geometry, it is to solve problems relating to the prediction of the geometry in unsampled geometrical fields. More specifically, it is a matter of using the *measure* as constraint of a process yielding a set of *quasi-infinite* numerical porous media. Our choice for $\sigma(r_x, r_y)$ is of course not random: in the fields of communications, electrical network analysis, defense systems, a variety of algorithms developed for generating random 1D signals with specified ACF and Probability Density Function (PDF) (Barrett, and Coales, 1955; Gujar, and Kavanagh, 1968; Holiday, 1969; Broste, 1970). Borrowing from this work, others, mainly Joshi (1974), generalized the theory to porous media. In the approach, a series of *quasi-infinite* binary numerical porous media are produced as the output of a random process constrained by a PDF (i.e., a porosity value for a 1–0 binary medium) and an ACF. The algorithm relies on linear and non-linear filters to tranform a set of Gaussian random numbers into a binary set with the desired porosity value and ACF. Thus it is now a common practice to generate *quasi-infinite* numerical porous media from acquired porosity value and ACF (Adler, 1992; Adler, Jacquin, and Quiblier, 1990; Giona, and Adrover, 1996; Ionnadis, Kwiecien, and Chatzis, 1997; Ionnadis and Lange, 1998; Quiblier, 1984; Sallés, Thovert, and Adler, 1994; Yao and others, 1993). In such a model, the porosity and the ACF characterize the structure of the process, e.g., the microgeometry of the numerical realizations. It becomes obvious that the demonstrated mathematical property of the ACF should have consequences on the practical use of such stochastic modeling. If the constraint fitted in the process is a measured ACF $\sigma(r_x, r_y)$, the random process cannot impose $\sigma(r_x, r_y)$ exactly in the different stochastic realizations: for a kth realization, one has inequality (21):

$$\sigma^k_{\text{synthetic}}(r_x, r_y) \neq \sigma(r_x, r_y) \tag{21}$$

where $\sigma^k_{\text{synthetic}}(r_x, r_y)$ is the ACF of a kth realization of the random process.
Equation (20) yields

$$\sigma^k_{\text{synthetic}}(r_x, r_y) = \sigma^{\text{intrinsic}}(r_x, r_y) + \delta\sigma^k_{\text{synthetic}}(r_x, r_y) \neq \sigma^{\text{intrinsic}}(r_x, r_y) + \delta\sigma(r_x, r_y) \tag{22}$$

where $\delta\sigma^k_{\text{synthetic}}(r_x, r_y)$ expresses that the stochastic process cannot impose exactly $\sigma(r_x, r_y)$ in a kth realization as a consequence the unicity of the pair binary image/$\sigma(r_x, r_y)$ and $\delta\sigma^k_{\text{synthetic}}(r_x, r_y)$ relates here to the existence of an uncontrolled structural noise generated by the stochastic process in a kth realization.

To correctly interpret the relation between the permeability tensor $\underset{\approx}{K}$ and the microgeometry [Eqs. (8) and (9)], it is necessary to verify that the structural noise does not control the output $\underset{\approx}{K}$ of the simulation. Depending on the impact of $\delta\sigma_{\text{synthetic}}^{k}(r_x, r_y)$ on any physical property, the use of the generator may be declared appropriate or not. In the second paper of this series, a review of the aforementioned generator (Joshi, 1974) will be provided. The existence of a structural noise, generated by the stochastic process in a series of realizations, will be highlighted.

ACKNOWLEDGMENTS

REFERENCES

Adler, P. M., 1992, Porous media: Butterworth, Heinemann, London, 544 p.

Adler, P. M., Jacquin, C. G., and Quiblier, J. A., 1990, Flow in simulated porous media: Int. J. Multiphase Flow, v. 16, no. 4, p. 691–712.

Anderson, T. B., and Jackson, R., 1967, A fluid mechanical description of fluidized beds: Ind. Eng. Chem. Fundam., v. 6, p. 527–538.

Anguy, Y., Bernard, D., and Ehrlich, R., 1994, The local change of scale method for modeling flow in natural porous media (I): Numerical tools: Adv. Water Resour., v. 17, p. 337–351.

Anguy, Y., Bernard, D. and Ehrlich, R., 1996, Towards realistic flow modeling. Creation and evaluation of two-dimensional simulated porous media: An image analysis approach: Surv. Geophys., v. 17, p. 365–287.

Anguy, Y., Ehrlich, R., Prince, C. M., Riggert, V., and Bernard, D., 1994, The sample support problem for permeability assessment in sandstone reservoirs, in Yarus, J. M. and Chambers, R. L., eds., Stochastic modeling and geostatistics: Am. Assoc. Petroleum Geologists Publication, Tulsa, NE, p. 37–54.

Bachmat, Y., and Bear, J., 1986, Macroscopic modeling of transport phenomena in porous media 1. The continuum approach: Trans. Porous Media, v. 1, p. 213–240.

Bakke, S., and Oren, P.-E., 1997, 3-D pore-scale modeling of sandstones and flow simulations in the pore networks: SPE J., v. 2, p. 136–149.

Barrére, J., Gipouloux, O., and Whitaker, S., 1992, On the closure problem for Darcy's law: Transp. Porous Media, v. 7, p. 209–222.

Barrett, J. F., and Coales, J. F., 1955, An introduction to the analysis of non-linear control systems with random inputs: Proc. IEEE Monogr. 154 M, p. 190–199.

Bear, J., 1972, Dynamics of fluids in porous media: Elsevier, New York, 796 p.

Bensoussan, A., Lions, J. L., and Papanicolaou, G., 1978, Asymptotic analysis for periodic structures: North Holland, New York.

Berg, R. R., 1975, Capillary pressure in stratigraphic traps: Am. Assoc. Petroleum Geol. Bull., v. 59, no. 6, p. 939–956.

Brenner, H., 1980, Dispersion resulting from flow through spatially porous media: Trans. R. Soc. (Lond.), v. 297, p. 81–133.

Brigham, E. O., 1974, The fast Fourier transform: Prentice-Hall, Englewood Cliffs, NJ, 252 p.

Broste, N. A., 1970, Digital generation of random sequences with specified autocorrelation and probability density functions: Report no. RE-TR-70-5, Advanced Sensors Laboratory, Research and Engineering Directorate, U.S. Army Missile Command, Redstone Arsenal, AL.

Bryant, S. L., King, P. R., and Mellor, D. W., 1993, Network model evaluation of permeability and spatial correlation in a real random sphere packing: Transp. Porous Media, v. 11, 53–70.

Carbonell, R. G., and Whitaker, S., 1984, Heat and mass transfer in porous media, *in* Bear, J., and Corapcioglu, M. Y., eds., Fundamentals of transport phenomena in porous media: Martinus Nijhoff, Dordrecht, The Netherlands, p. 121–198.

Cushman, J. H., 1990, An introduction to hierarchical porous media, *in* Cushman, J. H., ed., Dynamics of fluids in hierarchical porous media: Academic Press, New York, p. 1–6.

Dagan, G., 1979, The generalization of Darcy's law for non uniform flows: Water Resour. Res., v. 15, p. 1–7.

Dagan, G., 1990, Flow and transport in porous formations: Springer-Verlag, New York, 465 p.

Dullien, F. A. L., 1979, Porous media—Fluid transport and pore structure: Academic Press, New York, 396 p.

Ehrlich, R., Crabtree, S. J., Horkowitz, K. O., and Horkowitz, J. P., 1991a, Petrography and reservoir physics I: Objective classification of reservoir porosity: Am. Assoc. Petroleum. Geol. Bull., v. 75, no. 10, p. 1547–1562.

Ehrlich, R., Etris, E. L., Brumfield, D., Yan, L. P. and Crabtree, S. J., 1991b, Petrography and reservoir physics III: Physical models for pemeability and formation factor: Am. Assoc. Petroleum Geol. Bull., v. 75, no. 10, p. 1579–1592.

Ferreol, B., and Rothman, D. H., 1995, Lattice–Boltzmann simulations of flow through Fontainebleau sandstone: Transp. Porous Media, v. 20, p. 3–20.

Fienup, J. R., 1982, Phase retrieval algorithms: A comparison: Appl. Opt., v. 21, p. 2758–2769.

Fienup, J. R., and Wackerman, C. C., 1986, Phase retrieval stagnation problems and solutions: J. Opt. Soc. Am. A, v. 3, p. 1897–1907.

Garboczi, E. J., 1990, Permeability, diffusivity, and micro-structural parameters: A critical review: Cement Concrete Res., v. 20, p. 591–601.

Gelhar, L. W., 1984, Stochastic analysis of flow in heterogeneous porous media, *in* Bear, J., and Corapcioglu, M. Y., eds., Fundamentals of transport phenomena in porous media: Martinus Nijhoff, Dordrecht, The Netherlands, p. 615–717.

Gerchberg, R. W., and Saxton, W. O., 1972, A practical algorithm for the determination of phase from image and diffraction plane pictures: Optik, v. 35, 237–246.

Giona, M. and Adrover, A., 1996, Closed-form solution for the reconstruction problem in porous media: AIChE J., v. 42, no. 5, p. 1407–1415.

Graton, L. C., and Fraser, H. J., 1935, Systematic packing of spheres with particular relation to porosity and permeability: J. Geol., v. 43, p. 785–909.

Gray, W. G., 1975, A derivation of the equations for multiphase transport: Chem. Eng. Sci., v. 30, p. 229–233.

Gujar, U. G., and Kavanagh, R. J., 1968, Generation of random signals with specified probability density function and power density spectra: IEEE Trans. Automatic Control, p. 716–719.

Holiday, E. M., 1969, Transformation of a set of pseudo-random numbers into a set representing any desired probability and correlation: Report no. RE-TR-69-25, Advanced Sensors Laboratory, Research and Engineering Directorate, U.S. Army Missile Command, Redstone Arsenal, AL.

Ionnadis, M. A., Kwiecien M. J., and Chatzis, I., 1997, Electrical conductivity and percolation aspects of statistically homogeneous porous media: Transp. Porous Media, v. 29, p. 61–83.

Ionnadis, M. A., and Lange, E., 1998, Micro-geometry and topology of statistically homogeneous porous media, *in* Burganos, V. N., Karatzas, G. P., Payatakes, A. C., Brebbia, C. A., Gray, W. G., and Pinder, G. F., eds., Proceedings of computational methods in water resources XII, v. 1: Computational Mechanics Southampton, UK, p. 223–230.

Joshi, M. Y., 1974, A class of stochastic models for porous pedia: PhD Dissertation, University of Kansas, 154 p.

Kim, W., and Hayes, M. H., 1990, Phase retrieval using two Fourier-transform intensities: J. Opt. Soc. Am. A, v. 7, no. 3, p. 441–449.

Kwiecien, M. J., Macdonald, I. F. and Dullien, F. A. L., 1990, Three-dimensional reconstruction of porous media from serial section data: J. Microsc., v. 159, no. 3, p. 343–359.

Lane, R. G., 1987, Recovery of complex images from Fourier magnitudes: Optics commun., v. 63, no. 1, p. 6–10.

Marle, C. M., 1967, Ecoulements monophasiques en milieux poreux: Revue Institut Français du Pétrole, v. 22, p. 1471–1509.

Matheron, G., 1965, Les variables régionalisées et leur estimation: Masson & Cie, Paris, 305 p.

Matheron, G., 1970, La théorie des variables régionalisées, et ses applications: Les Cahiers du Centre de Morphologie de Fontainebleau, v. 5, Ecole des Mines de Paris, eds., Paris, 212 p.

McCreesh, C. A., Ehrlich, R. and Crabtree, S. J., 1991, Petrography and reservoir physics II: Relating thin section porosity to capillary pressure curves, the association between pore types and throat size: Am. Assoc. Petroleum Geol. Bull., v. 75, no. 10, p. 1563–1578.

Millane, R., 1990, Phase retrieval in crystallography and optics: J. Opt. Soc. Am. A, v. 7, no. 3, p. 394–411.

Nieto-Vesperinas, M., 1993, A Fortran routine to estimate a function of two variables form its autocor-relation: Comput. Phys. Commun., v. 78, p. 211–217.

Nozad, I., Carbonell, R. G., and Whitaker, S., 1985, Heat conduction in multiphase systems—1: Theory and experiment for two-phase systems: Chem. Eng. Sci., v. 40, no. 5, p. 843–855.

Pérez-Ilzarbe, M. J., 1992, Phase retrieval from the power spectrum of a periodic objet: J. Opt. Soc. Am. A, v. 9, no. 12, p. 2138–2148.

Pérez-Ilzarbe, M. J., Nieto-Vesperinas, N., and Navarro, R., 1990, Phase retrieval from experimental far-field intensity data: J. Opt. Soc. Am. A, v. 7, no. 3, p. 434–440.

Pilotti, M., 1998, Generation of realistic porous media by grains sedimentation: Transp. Porous Media, v. 33, p. 257–278.

Prat, M., 1990, Modelling of heat transfer by conduction in a transition region between a porous medium and an external fluid: Transp. Porous Media, v. 5, p. 71–95.

Prince, C. M., and Ehrlich, R., 1990, Analysis of spatial order in sandstones I: Basic principles: Math. Geol., v. 22, no. 3, p. 333–359.

Prince, C. M., Ehrlich, R. and Anguy, Y., 1995, Analysis of spatial order in sandstones II: Grain clusters, packing flaws and the small-scale structure of sandstones: J. Sedim Res., v. A65, p. 13–28.

Quiblier, J. A., 1984, A new three-dimensional modeling technique for studying porous media: J. Colloid Interface Sci., v. 98, no. 1, p. 84–101.

Quintard, M., and Whitaker, S., 1987, Ecoulement monophasique en milieu poreux: effets des hétérogéités locales: J. de Mécanique Théorique et Appliquée, v. 6, no. 5, p. 691–726.

Quintard, M., and Whitaker, S., 1990, Two-phase flow in heterogeneous porous media I: The influence of large spatial and temporal gradients: Transp. Porous Media, v. 5, p. 341–379.

Quintard, M., and Whitaker, S., 1993, Transport in ordered and disordered porous media: Volume-averaged equations, closure problems, and comparison with experiment: Chem. Eng. Sci., v. 48, no. 14, p. 2537–2564.

Quintard, M., and Whitaker, S., 1994a, Transport in ordered and disordered porous media I: The cellular average and the use of weighting functions: Transp. Porous Media, v. 14, p. 163–177.

Quintard, M., and Whitaker, S., 1994b, Transport in ordered and disordered porous media II: General-ized volume-averaging: Transp. Porous Media, v. 14, p. 179–206.

Quintard, M., and Whitaker, S., 1994c, Transport in ordered and disordered porous media III: Closure and comparison between theory and experiment: Transp. Porous Media, v. 15, p. 31–49.

Quintard, M., and Whitaker, S., 1994d, Transport in ordered and disordered porous media IV: Computer generated porous media for three-dimensional systems: Transp. Porous Media, v. 15, p. 51–70.

Quintard, M. and Whitaker, S., 1994e, Transport in ordered and disordered porous media V: Geometrical results for two-dimensional systems: Transp. Porous Media, v. 15, p. 183–196.

Renard, P., and de Marsily, G., 1997, Calculating equivalent permeability: A review: Adv. Water Resour., v. 20, no. 5–6, p. 253–278.

Roddier, F., 1985, Distributions et transformation de Fourier: McGraw-Hill, Paris, 323 p.

Rubinstein, J., and Torquato, S., 1989, Flow in random porous media: Mathematical formulation; variational principles and rigorous bounds: J. Fluid Mech., v. 206, p. 3–25.

Sallés, J., Thovert, J. F., and Adler, P. M., 1994, Transport in reconstructed porous media, *in* Rouquerol, J., and others, eds., Studies in surface science and catalysis, v. 87: Elsevier, Amsterdam, p. 211.

Sanchez-Palencia, E., 1980, Non homogeneous media and vibrational theory: Springer-Verlag, Berlin.

Sasaki, O., and Yamagami, T., 1987, Phase retrieval algorithms for nonnegative and finite-extent objects: J. Opt. Soc. Am. A., v. 4, no. 4, p. 720–726.

Sault, R. J., 1984, Two procedures for phase estimation form visibility magnitudes: Aust. J. Phys., v. 37, p. 209–229.

Saxton, W. O., 1978, computer techniques for image processing in electron microscopy: Advances in Electronics and Electron Physics, Suppl. v. 10., Academic Press, New York.

Schultz, T. J., and Snyder, D. L., 1992, Image recovery from correlations: J. Opt. Soc. Am. A., v. 9, no. 8, p. 1266–1272.

Slattery, J. C., 1967, Flow of viscoelastic fluids through porous media: AIChE, v. 13, p. 1066–1077.

Tartar, L., 1980, Incompressible fluid flow in a porous medium: Convergence of the homogeneization process, *in* Lecture notes in physics 127, Appendix 2: Springer-Verlag, New York.

Thovert, J. F., Sallés, J., and Adler, P. M., 1992, Computerized characterization of the geometry of real porous media: Their discretization, analysis and interpretation: J. Microsc., v. 170, p. 65–79.

van Brakel, J., 1975, Pore space models for transport phenomena in porous media. Review and evaluation with special emphasis to capillary liquid transport: Powder Technol., v. 11, p. s205–236.

Ventzel, H., 1973, Théorie des probabilités: MIR, Moscou, 584 p.

Weathcraft, S. W., Sharp, G. A., and Tyler, S. W., 1990, Fluid flow and solute transport in fractal heterogeneous porous media, *in* Cushman, J. H., ed., Dynamics of fluids in hierarchical porous media: Academic Press, San Diego, CA, p. 305–326.

Whitaker, S., 1967, Diffusion and dispersion in porous media: AIChE, v. 13, p. 420–427.

Whitaker, S., 1969, Advances in the theory of fluid motion in porous media: Ind. Eng. Chem, v. 61, p. 14–28.

Whitaker, S., 1986, Flow in porous media I: A theoretical derivation of Darcy's law: Transp. Porous Media, v. 1, p. 3–25.

Yao, J., Frykman, P., Kalaydjian, F., Thovert, J. F., and Adler, P. M., 1993, High-order moments of the phase function for real and reconstructed porous media: A comparison: J. Colloid. Interface. Sci., v. 146, p. 478.